

A feedback SIR (fSIR) model highlights advantages and limitations of infection-dependent mitigation strategies

Elisa Franco,
Department of Mechanical and Aerospace Engineering,
Department of Bioengineering,
Molecular Biology Institute,
University of California, Los Angeles

December 24, 2020

Abstract

Transmission rates in epidemic outbreaks vary over time depending on the societal and government response to infections and mortality of the disease. Non-pharmacological mitigation strategies such as social distancing and the adoption of protective equipment aim precisely reducing transmission rates by reducing infectious contacts. To investigate the effects of mitigation strategies on the evolution of epidemics, nonlinear transmission rates that are influenced by the levels of infections, deaths or recoveries have been included in many variants of the classical SIR model. This class of models is particularly relevant to the COVID-19 epidemic, in which the population behavior has been affected by the unprecedented abundance and rapid distribution of global infection and death data through online platforms. This manuscript revisits a SIR model in which the reduction of transmission rate is due to knowledge of infections. Through a mean field approach that assumes individuals behave like molecules in a well-mixed solution, one derives a time-varying reproduction number that depends on infection information through a negative feedback term that is equivalent to Holling type II functions in ecology and Michaelis-Menten functions in chemistry and molecular biology. A step-by-step derivation of the model is provided, together with an overview of methods for its qualitative analysis, showing that negative feedback structurally reduces the peak of infections. At the same time, feedback may substantially extend the duration of an epidemic. Computational simulations agree with the analytical predictions, and further suggest that infection peak reduction persists even in the presence of information delays. If the mitigation strategy is linearly proportional to infections, a single parameter is added to the SIR model, making it useful to illustrate the effects of infection-dependent social distancing.

1 Introduction

Compartment models are widely used to capture the long-term temporal evolution of epidemic outbreaks. Like mean-field models in physics and chemistry, compartment models assume a well-mixed population and capture average interactions patterns. The population is binned in distinct categories (the compartments), that at a minimum include those susceptible to disease (S), those who become infected (I), and those who recover (R), like in the well-known SIR model by Kermack and McKendrick (Kermack and McKendrick, 1927; Hethcote, 2000). Because the SIR model is not suited to capture epidemics with a long incubation time, a large population of asymptomatic individuals, and high lethality, many SIR variants with additional compartments have been developed and tailored to model specific epidemic outbreaks (Capasso and Serio, 1978; Bootsma and Ferguson, 2007; Giordano et al., 2020). In the context of the COVID-19 pandemic, SIR-like models have been used to forecast local outbreaks (Bertozzi et al., 2020) and to formulate recommendations for suppression and mitigation strategies (Kruse and Strack, 2020; Bin et al., 2020; Casella, 2020; Della Rossa et al., 2020).

As the capacity of COVID-19 testing has increased, infection, recovery, and death data have become available at the local and global level with unprecedented speed thanks to online dashboards, apps, and media reports (Dong et al., 2020a; Rosini, 2020; Prasse et al., 2020). This information has influenced the behavioral choices of the public, and has been essential for governments to make critical decisions in regards to suppression and mitigation policies. While these policies can successfully quench the epidemic with an *open loop* approach that discounts recent data (Bin et al., 2020; Sadeghi et al., 2020), strategies that respond in *closed loop* to trends in the current level of infections, deaths, or recoveries are more likely to be accepted or even spontaneously adopted by the population.

Compartment models have been adapted to capture the effects of societal responses (such as mitigation strategies, behavioral changes, and vaccinations) that are influenced in *closed loop* by epidemic information. This has been done by introducing nonlinear transmission functions, also known as “behavioral functions”, which are chosen empirically to be smooth threshold/saturation or polynomial functions (Capasso and Serio, 1978; Anderson and May, 1978; Korobeinikov, 2006). One of the first contributions in this area is the SIR model variant described by Capasso and Serio to describe the cholera epidemics in Bari in 1973, in which the transmission rate includes a general nonlinear function of infections (Capasso and Serio, 1978). This function is further specified to decrease and saturate as infections increase, like Michaelis-Menten rates in biochemistry and Holling type II functions in ecology. The general influence of nonlinear transmission rates on the equilibria and dynamics of similar models were examined in (Liu et al., 1986, 1987), and more recently in (Korobeinikov and Maini, 2005; Kyrychko and Blyuss, 2005; Li and Zhang, 2017; Chapwanya et al., 2012; Kumar et al., 2020). Bootsma and Ferguson adopted a SEIR model in which a nonlinear Michaelis-Menten term captures the effects of death awareness on social interactions during the 1918 influenza epidemic in the United States (Bootsma and Ferguson, 2007). Similarly, SIS, SIR, and SEIRS models have been modified to capture the reduction of trans-

mission and contact rates achieved by infection awareness programs (Greenhalgh et al., 2015; Samanta and Chattopadhyay, 2014; Yu et al., 2017). These models have also examined how infection awareness can reduce the susceptible fraction of the population (Kiss et al., 2010; Funk et al., 2009), in particular by increasing vaccination rates (Buonomo et al., 2008).

This manuscript revisits, examines, and provides some novel results on a class of modified SIR models originally described by (Capasso and Serio, 1978), in which the infection-dependent transmission rate introduces a feedback loop. Rather than being adopted based on empirical observations, here the nonlinear transmission rate is derived step-by-step using the law of mass action. It is assumed that individuals behave like particles in a well-mixed solution, and their interactions are modeled through equivalent chemical reactions that can be converted to ordinary differential equations (ODEs) by applying the law of mass action. Mitigation strategies such as social distancing and use of protective equipment are modeled as reactions that reduce successful infections at a rate that depends on current infection levels. Through a quasi-steady state argument, one obtains a nonlinear transmission rate parameter that includes a specific “mitigation function” term and is comparable to Michaelis-Menten functions. This approach produces a SIR model similar to the one described in (Section 6, (Capasso and Serio, 1978)). Because the nonlinear transmission function decreases as a function of infections, a *negative* feedback loop emerges and it is convenient to adopt the nomenclature feedback SIR (fSIR).

Most nonlinear epidemic models are positive and structurally bounded; stability analysis of the equilibria can be done via local (linearization) or global methods (typically Lyapunov functions), obtaining conditions for convergence to a disease-free equilibrium, or conditions for the occurrence of bifurcations in the presence of an endemic equilibrium (in which a fraction of the population remains infected) (Liu et al., 1987; Korobeinikov and Maini, 2005; Kyrychko and Blyuss, 2005; Greenhalgh et al., 2015; Weitz et al., 2020). Here the equilibria and the solutions of the fSIR model are examined (through established approaches) with focus on comparing the outcome in the presence and in the absence of mitigation. Specifically, I show that a broad class of infection-dependent mitigation functions makes it possible to reduce the peak of infections for any mitigation intensity. If the mitigation function depends linearly on infections, it is shown that the peak is also postponed for all positive mitigation parameters. These benefits of mitigation are however counterbalanced by the fact that the duration of the epidemic, measured as the time for which infections persist, may significantly increase – an effect that is demonstrated with a simple linear approximation. Computational simulations support the analysis reported, and indicate that mitigation of the peak persists even in the presence of delay in the transmission of infection information, which induces a moderate retardation of the time at which infections peak. Finally, for purely illustrative purposes, I highlight that the fSIR model can qualitatively capture infection data of the COVID-19 pandemic for countries like the United Kingdom, the United States and Sweden, that opted for mitigation rather than suppression.

This brief study of the fSIR model shows that it is a helpful tool to illustrate the effects of mitigation strategies in epidemics, with particular relevance to the COVID-19 epidemic that is characterized by rapid spread of information and fluctuations in

social distancing patterns. While more complex models and data-driven parameter estimation are clearly needed for epidemic prediction (Anastassopoulou et al., 2020; Giordano et al., 2020; Calafiore et al., 2020), simple yet rigorous models like the fSIR are valuable as they provide qualitative insights. Only one term, the mitigation function, is needed in addition to the reproduction number to describe the evolution of the epidemic in the presence of infection-based mitigation strategies. This term reduces to a single parameter in the special case in which the mitigation strategy is a linear function of infections. Further, this model supports mitigation guidelines as it clearly shows that the infection curve can be flattened without postponing the peak, a misleading (and demotivating) scenario suggested by similar models that use a constant transmission rate. At the same time, the model highlights that policies relying exclusively on infection data to regulate social distancing can majorly extend the time required to reach a disease-free equilibrium.

1.1 Background: qualitative analysis of the non-dimensional SIR model

The well-known SIR model is reviewed in this section to establish notation and background concepts (Hethcote, 2000). It is assumed that the total population remains constant (birth and death processes are neglected) and the dynamics are driven by two key parameters:

1) the disease transmission coefficient β , which depends on the social interactions among individuals (average daily contacts) and on the infection characteristics; the transmission rate is generally thought as the product of the average frequency of contacts between infected and susceptible and the likelihood that infection occurs given a contact;

2) the recovery coefficient γ , which captures the average time for recovery (or death) of infected individuals. The inverse $1/\gamma$ is also known as duration of infectiousness. Assuming the total population is N , the original SIR model is:

$$\frac{dS}{dt} = -\frac{\beta}{N}IS, \quad (1)$$

$$\frac{dI}{dt} = \frac{\beta}{N}IS - \gamma I, \quad (2)$$

$$\frac{dR}{dt} = \gamma I. \quad (3)$$

For simplicity, here we do not model the possibility of reinfection of recovered individuals (Hethcote, 1976). The transmission coefficient is normalized by the total population size, because the number of new infections per unit time occur based on the average infectious contacts of each susceptible individual and does not depend on the total population size (this is also called standard incidence (Hethcote, 2000, 1976)). Because the total population is assumed to remain constant, at any point in time $R = N - I - S$ and the model can be reduced to two ordinary differential equations (ODEs). Further, the variables can be normalized by the total population setting $s = S/N$, $i = I/N$ (and $r = R/N$); by rescaling time as $\tau = t\gamma$, the

SIR model becomes non-dimensional, with a single coefficient $\mathcal{R}_0 = \beta/\gamma$, the well known reproduction ratio or reproduction number (Hethcote, 1976).

$$\frac{ds}{d\tau} = -\mathcal{R}_0 i s, \quad (4)$$

$$\frac{di}{d\tau} = (\mathcal{R}_0 s - 1)i. \quad (5)$$

Given initial conditions $s_0 = s(0)$ and $i_0 = i(0)$, the solutions $s(\tau)$ and $i(\tau)$ will be generally denoted as s and i with the assumption that these symbols indicate functions of time (unless otherwise noted). It is well-known that the solutions are non-negative and satisfy the conservation law $s + i + r = 1$ (Hethcote, 1976). Exact expressions for the solution have been computed (Harko et al., 2014). If there are no infected individuals ($i_0 = 0$), the system remains in the equilibrium $E_0 = (s_0, 0, r_0)$ because all derivatives are identically zero. For any initial value of infections $i_0 > 0$, the solutions s and i are bounded and evolve in the invariant set $\mathcal{P} = \{0 \leq s \leq s_0, 0 \leq i \leq 1, 0 \leq r \leq 1\}$. This follows from the fact that $ds/d\tau \leq 0$, so $s(\tau) \leq s_0, \forall \tau \geq \tau_0$. The solutions and the admissible equilibria depend on the value of \mathcal{R}_0 and on the initial value of the susceptible population s_0 .

Case 1: $\mathcal{R}_0 s_0 = 0$. This occurs when the transmission rate or the initial susceptible population are equal to zero. In either case, $s(t)$ remains identically zero; $di/d\tau \leq 0$ becomes a linear asymptotically stable equation with zero as the only equilibrium.

Case 2: $\mathcal{R}_0 s_0 < 1$. In this case the infected population is non-increasing because $di/d\tau \leq 0$, thus the epidemic does not start (the system reaches an equilibrium $\tilde{E} = (\tilde{s}, 0, \tilde{r})$).

Case 3: $\mathcal{R}_0 s_0 < 1$. In this case $di/d\tau$ initially increases, reaches a peak when $s = s_{crit} = 1/\mathcal{R}_0 \leq s_0$, and finally decreases to zero. The equilibrium in this case is $E = (\bar{s}, 0, \bar{r})$. Because $s_0 \leq 1$, $\mathcal{R}_0 s_0 > 1 \Rightarrow \mathcal{R}_0 > 1$. For any positive i_0 and $\mathcal{R}_0 s_0 > 1$, the relation between susceptible and infected can be computed exactly from the ratio of $di/d\tau$ and $ds/d\tau$ (Hethcote, 1976):

$$\frac{di}{ds} = \frac{\mathcal{R}_0 s - 1}{-\mathcal{R}_0 s} = -1 + \frac{1}{\mathcal{R}_0 s} \Rightarrow di = -ds + \frac{ds}{\mathcal{R}_0 s}.$$

Integrating we obtain the relation between i and s :

$$i = i_0 + s_0 - s - \frac{1}{\mathcal{R}_0} \log \frac{s_0}{s}. \quad (6)$$

The peak of infections occurs when $s = s^* = 1/\mathcal{R}_0$ ($s = s^*$ yields $di/d\tau = 0$). Substituting s^* we find:

$$i_{max} = i_0 + s_0 - \frac{1}{\mathcal{R}_0} (1 + \log(s_0 \mathcal{R}_0)), \quad (7)$$

with $\log(s_0 \mathcal{R}_0) > 0$ because $s_0 \mathcal{R}_0 > 1$ (we assume that prior to the start of the epidemic the recovered population is zero, thus $i_0 + s_0 = 1$). From expression (6),

by setting $\bar{i} = 0$, we can also derive an implicit equation to find the equilibrium value of the susceptible population:

$$\log \frac{s_0}{\bar{s}} = \mathcal{R}_0(1 - \bar{s}), \quad (8)$$

which has one positive root (because $\bar{s} < s_0 \leq 1$ and $\mathcal{R}_0 > 1$). In other words, the equilibrium susceptible population is positive (not all the population has become infected), unless \mathcal{R}_0 is unrealistically large.

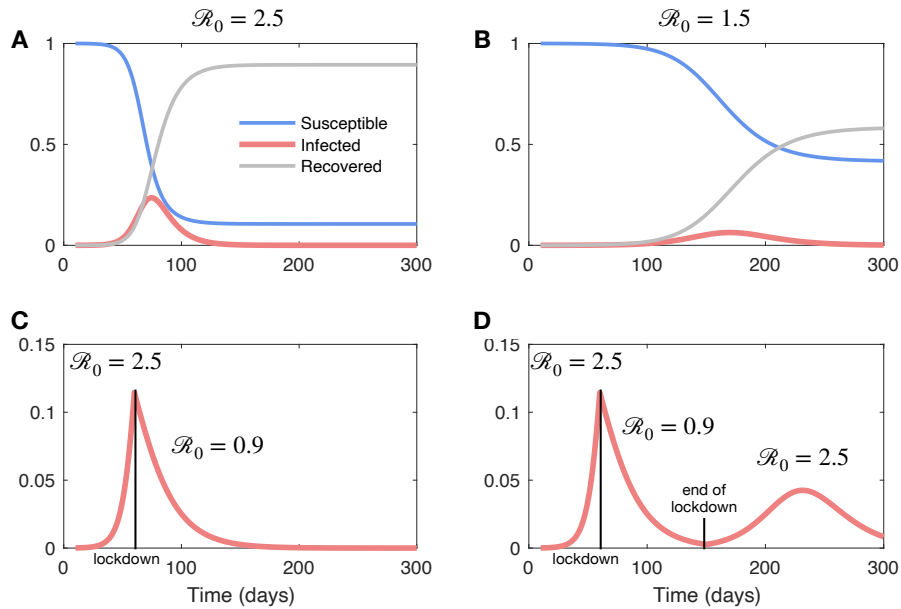


Figure 1: A and B: Illustrative computational simulations showing the SIR dynamics for different values of (constant) reproduction coefficient \mathcal{R}_0 . The plot in B illustrates how a lower value of \mathcal{R}_0 “flattens the curve” while also significantly delaying the infection peak. This illustration may be misleading to the public, because the introduction of suppression or mitigation measures causes the transmission rate constant \mathcal{R}_0 to vary in time. C: A lockdown scenario in which \mathcal{R}_0 switches from 2.5 to 0.9 after day 60. D: Lifting the lockdown at day $t_{\text{end}} = 150$ causes the infections to increase again ($s(t_{\text{end}})\mathcal{R}_0 > 1$).

1.2 Flattening and reshaping the infection curve through suppression and mitigation policies

The SIR model has been often used during the COVID-19 pandemic to illustrate how a low reproduction number \mathcal{R}_0 (or a low transmission rate β) has the effect

of “flattening the (infection) curve”, *i.e.* reducing the infection peak while extending the duration of the epidemic. The simulations in Fig. 1 A and B compare the SIR solutions for values of $\mathcal{R}_0 = 2.5$, which is close to recent estimates for the COVID-19 outbreak (Kucharski et al., 2020), and $\mathcal{R}_0 = 1.5$. The infection peak is clearly reduced when $\mathcal{R}_0 = 1.5$, however the infection peak is also significantly delayed. The reproduction number depends on many factors, including societal habits and pharmacological interventions. In 2020, reducing the reproduction number of COVID-19 is only possible by controlling societal interactions, given the lack of approved vaccines and standardized medical treatment protocols (Stewart et al., 2020).

Suppression (lockdown) or mitigation (social distancing and adoption of Personal Protective Equipment, PPE) policies aiming to control and extinguish the epidemic may fluctuate over time to minimize their impact on society, thereby introducing fluctuations of \mathcal{R}_0 (Stewart et al., 2020). While useful to illustrate the concept and the effects of the reproduction number, Figs 1 A and B do not represent temporal changes of \mathcal{R}_0 and are thus misleading to the public and to policymakers. During the COVID-19 epidemic, enormous research efforts are dedicated to a continuous estimation and forecasting of the reproduction number as a function of societal response (Giordano et al., 2020; Bertozzi et al., 2020; Anastassopoulou et al., 2020; Kissler et al., 2020).

As of mid 2020, the most successful strategy to manage COVID-19 was full suppression of social interactions (lockdown); states such as China, South Korea, Italy, Spain, and France went on strict lockdown for more than two months, containing infections by Summer 2020. Qualitatively, the effects of a lockdown can be captured by a SIR model in which \mathcal{R}_0 rapidly changes from a high to a low value; the simulation in Fig. 1C illustrates the profile of infections under an abrupt change of \mathcal{R}_0 from 2.5 to 0.9 after 60 days from the start of the epidemic; the disease-free equilibrium is reached within a few months from the start of the suppression. However, ending lockdown measures too early can cause the epidemic to restart if $s(t_{\text{end}})\mathcal{R}_0 > 1$, as illustrated in Fig. 1D, where the lockdown is completely lifted after 90 days (Bertozzi et al., 2020). The success of lockdown is also tied to the ability to coordinate regulations and enforcement, and to sustain its major impact on the economy and on the mental health of the population. Due to the significant upfront “cost”, lockdowns are unpopular and difficult to enforce.

Mitigation strategies have been adopted in many countries during the COVID-19 pandemic as a complement or replacement to lockdowns, and are thus an important phenomenon that should be included in mathematical models. Mitigation means the reduction of large-scale public events, closure of certain businesses, and safe-at-home orders that could be classified as social distancing; mitigation efforts include the use of PPE such as masks, face shields, and gloves. Mitigation policies may become more restrictive or relax over time, depending on fluctuations of the contagion data, and on social and political climate. Restrictions to social interactions are likely to be more effective if they are tied to the reported infections or deaths, which increase the perceived risk of infection. With fast spread of information about testing results (Dong et al., 2020a; Rosini, 2020; Prasse et al., 2020), knowledge of *infections* may be more helpful than deaths in quickly containing epi-

demics; because the average time to death for COVID-19 patients, for example, is 17 days (Zhou et al., 2020), reliable lethality information may only be available with a significant delay.

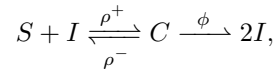
The rest of this manuscript derives and revisits an SIR model that qualitatively captures mitigation strategies and societal responses based on knowledge of infections, which introduce feedback in the epidemic process.

2 Results

2.1 Mitigation policies yield nonlinear transmission rate parameters

Here I provide a simple step-by-step derivation of a SIR model in which the transmission rate parameter varies as a function of infection-based mitigation policies, reproducing the empirical model described by (Capasso and Serio, 1978). It is assumed that individuals behave like molecules in a well-mixed solution and interact through equivalent chemical reactions. The corresponding ODEs are derived using the law of mass action in chemistry. A related mean-field approach, that considers individuals as agents that interact with a limited foraging radius has been considered in (Kolokolnikov and Iron, 2020), obtaining an exponential saturating transmission rate. In the context of predator-prey models, in (Dawes and Souza, 2013) the population-level Holling's functional responses is derived in a limit scenario starting from individual-level stochastic interactions.

First, a contagion may occur when a susceptible individual (S) and an infected individual (I) are in spatial proximity for some time (associated or contact state C); this encounter may then result in two infected individuals. This can be modeled using the equivalent chemical reactions:



where ρ^+ and ρ^- are the rates of association and dissociation of a susceptible and an infected individual, and we can associate ϕ with the daily rate at which individuals that have been exposed become infected. The law of mass action converts reactions like the one above to ODEs in which variables are concentrations of reactants and products, computed by dividing the number of molecules by the reaction volume. Similarly, here one can derive an ODE for the fraction of individuals in each compartment by dividing the number of individuals by the total population. The ODE describing the kinetics of the fraction of individuals (c) in the associated state (C) is:

$$\frac{dc}{dt} = \rho^+ s \cdot i - (\rho^- + \phi)c.$$

Because contacts occur on an hourly or daily basis, which is much faster than timescale of the epidemic, it is sensible to assume $dc/dt = 0$ and derive an expres-

sion for the equilibrium level of associated individuals:

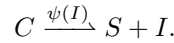
$$\bar{c} = \frac{\rho^+}{\rho^- + \phi} s \cdot i.$$

This value of \bar{c} is intended to represent a dynamic equilibrium at the population level, so it indicates the average number of contacts per day. With this definition, the transmission rate β introduced in model (1)-(2) is:

$$\beta = \frac{\rho^+ \phi}{\rho^- + \phi},$$

where ϕ is the probability of infection per contact, and $\rho^+ / (\rho^- + \phi)$ is the average number of contacts per day per individual, a definition that is consistent with the literature (Hethcote, 2000).^a The corresponding (non-dimensional) reproduction coefficient can be computed as earlier $\mathcal{R}_0 = \beta / \gamma$. Note that if $\rho = 0$ and ϕ is slow, with this approach we would recover the SEIR model (Hethcote, 2000), where the “contact” species C corresponds to the exposed category E . Here we will assume that the parameter ϕ is large enough that the contact \bar{c} can be neglected in the overall mass balance; if this were not the case, then \bar{c} must be explicitly included in the mass equation $s + i + \bar{c} + r = 1$.

In the presence of mitigation policies that discourage association of individuals, *i.e.* social distancing, the level of individuals in associated state C should decrease. This can be modeled by additional, fast dissociation process that depends on the known infection levels through a rate parameter $\psi(I)$:



For this to be a well-posed reaction, we require the distancing parameter $\psi(I)$ to be a non-negative, non-decreasing function of I , with $\psi(0) = 0$. With this model for dissociation, individuals in state c evolve according to the ODE:

$$\frac{dc}{dt} = \rho^+ s \cdot i - (\rho^- + \phi)c - \psi(i) \cdot c,$$

which equilibrates to:

$$\bar{c} = \left(\frac{\rho^+}{\rho^- + \phi} \right) \frac{1}{1 + \kappa(i)} s \cdot i, \quad \kappa(i) = \frac{\psi(i)}{\rho^- + \phi}.$$

With this equilibrium value for the average contacts, we derive a time-varying expression for the reproduction number that depends on the infection levels:

$$\mathcal{R}(i) = \mathcal{R}_0 \frac{1}{1 + \kappa(i)}. \quad (9)$$

^aThis definition of β can be verified by using the law of mass action to write the ODEs of s and i . For example

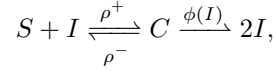
$$\frac{ds}{dt} = -\rho^+ s \cdot i - \rho^- c,$$

in which c has to be replaced by its equilibrium value \bar{c} .

The function $\kappa(i)$ is in units of /time/individual (or fraction of individuals, the equivalent of a normalized concentration in chemical reaction networks). Thus $\mathcal{R}(i)$ is non-dimensional like \mathcal{R}_0 .

Expression (9) is equivalent to Holling type II functions in ecology, and Michaelis-Menten/Hill functions in chemical kinetics, and indicates that under a policy in which social distancing depends on the infection levels, the reproduction number $\mathcal{R}(i)$ decreases as the infection numbers raise (Capasso and Serio, 1978; Bootsma and Ferguson, 2007; Li and Zhang, 2017). One can think about the feedback term $1/(1 + \kappa(i))$ as a reduction of the duration or frequency of infectious contacts introduced by social distancing policies.

Another successful approach to mitigate the spread of contagions is to recommend the use of PPE such as masks and gloves when the number of infected individuals increases. A simple way to model the average effect of PPE is to assume a change in the likelihood of infection following a contact:



with $\phi(I)$ being a decreasing function of the level of infections: the more contagions are known, the more widespread is the use of PPE, the lower the chance of becoming infected. One ought to assume that in the absence of information on infections, the natural infection probability is recovered, *i.e.* $\phi(0) = \phi$. A suitable function is:

$$\phi(I) = \frac{\phi}{1 + \xi(I)},$$

with $\xi(0) = 0$, and $\xi(I)$ non-negative, non-decreasing. With a timescale separation argument one can find the average daily level of (normalized) infectious contacts:

$$\bar{c} = \frac{\rho^+}{\rho^- + \xi(i)}.$$

With this expression, the time-varying reproduction number is:

$$\mathcal{R}(i) = \mathcal{R}_0 \frac{1}{1 + \kappa(i)}, \quad \kappa(i) = \frac{\rho^- \xi(i)}{\rho^- + \phi}.$$

This result is identical to equation (9) if we take $\xi(i) = \psi(i)/\rho^-$. For this reason, from now on we will use the time-varying reproduction number (9) as a general expression to model the effects of infection-aware mitigation on the dynamics of an epidemic. In the rest of the manuscript, $\kappa(i)$ will be called *mitigation function*.

2.2 The feedback SIR model

With infection-aware mitigation policies, the non-dimensional SIR model (4)-(5) becomes the feedback SIR (fSIR) model:

$$\frac{ds}{d\tau} = -\mathcal{R}_0 \frac{1}{1 + \kappa(i)} si = -\mathcal{R}(i)si \quad (10)$$

$$\frac{di}{d\tau} = \left(\mathcal{R}_0 \frac{1}{1 + \kappa(i)} s - 1 \right) i = (\mathcal{R}(i)s - 1)i. \quad (11)$$

In the fSIR model the transmission rate is the nonlinear function $\mathcal{R}(i) = \mathcal{R}_0 \frac{1}{1 + \kappa(i)}$; we assume the mitigation function $\kappa(i)$ is a non-negative, non decreasing function of i , with $\kappa(0) = 0$. For the simple case in which $\kappa(i) = \kappa i$ (mitigation function linearly proportional to infections), $\mathcal{R}(i)$ decreases monotonically as a function of i , and it decreases more steeply for large values of κ , as illustrated in Fig. 2. The larger κ , the smaller the value of i that induces a significant reduction in \mathcal{R}_0 (i.e. distancing and PPE are adopted in response to a very small outbreak). For example, a value of $\kappa = 2$ results in $\mathcal{R}(i) = \mathcal{R}_0/2$ when $i = 0.5$; a value of $\kappa = 10$ cuts in half \mathcal{R}_0 much sooner, when $i = 0.1$.

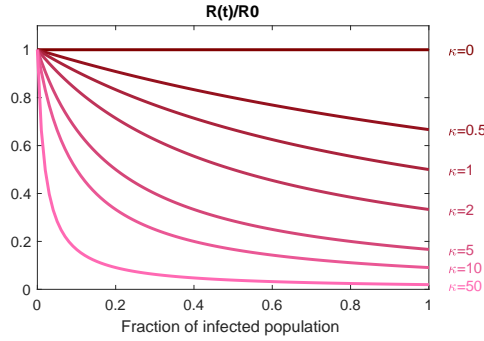


Figure 2: In the case of mitigation function linearly proportional to infections, $\kappa(i) = \kappa \cdot i$, the infection-dependent reproduction number (9) is monotonically decreasing as a function of infections, for any choice of $\kappa \geq 0$.

The mitigation function $\kappa(i)$ models the average population response to knowledge of current infection numbers, in relation to typical interaction patterns; this coefficient could also be used to model the collective “trust” in infection information. For $\kappa(i) = 0$, i.e. there is no reaction/policy, nor trust on infection data, then $\mathcal{R}(i) = \mathcal{R}_0$. (Similarly, if there are no infections and $i = 0$, then we have no change in $\mathcal{R}(i) = \mathcal{R}_0$ because $\kappa(0) = 0$).

The time varying reproduction number $\mathcal{R}(i)$ introduces a *negative* feedback loop in the epidemic model, because captures the fact that society mitigates interactions in response to an increase of infections, thereby reducing the reproduction number. This expression for $\mathcal{R}(i)$ also models the return to typical interaction patterns when infections are no longer present.

2.3 Properties of the fSIR model

2.3.1 Analysis of equilibria

Local equilibrium analysis and global stability analysis of SIR models with nonlinear transmission rates has been extensively carried out in the literature (Capasso and Serio, 1978; Liu et al., 1987; Korobeinikov and Maini, 2005). A brief discussion of the local stability of equilibria is reported below for illustrative purposes.

If $i_0 = 0$ ($r_0 = 0$), the system remain at the equilibrium $E_0 = (s_0, 0, 0)$ because all derivatives are identically zero. For any $0 < i_0 < 1$, the solutions are bounded and evolve in the invariant set $\mathcal{P} = \{0 \leq s \leq s_0, 0 \leq i \leq 1, 0 \leq r \leq 1\}$. If $\mathcal{R}_0 s_0 \leq 1 + \kappa(i_0)$, the infected population is non-increasing because $di/d\tau \leq 0$, the epidemic does not start and the system reaches an equilibrium $\bar{E} = (\bar{s}, 0, \bar{r})$. Like in the SIR model, because $s_0 \leq 1$, for the epidemic to start it is necessary that $\mathcal{R}_0 > 1 + \kappa(i_0)$.

If $\mathcal{R}_0 s_0 > 1 + \kappa(i_0)$, $di/d\tau > 0$ until the susceptible population decreases to the value $s = s_{crit} = (1 + \kappa(i_{max}))/\mathcal{R}_0 > \mathcal{R}_0$ at which $i(\tau) = i_{max}$. As the susceptible population continues to decrease, so does the infected population and the system reaches an equilibrium $E = (\bar{s}, 0, \bar{r})$.

Proposition 1 *Assume $\mathcal{R}_0 s_0 > 1 + \kappa(i_0)$. Any equilibrium $\bar{E} = (\bar{s}, 0, \bar{r})$ is locally stable.*

Proof The Jacobian of the fSIR model is:

$$J = \begin{bmatrix} -\bar{i}\mathcal{R}(\bar{i}) & -\bar{s}\frac{d}{di}\mathcal{R}(\bar{i}) \\ \bar{i}\mathcal{R}(\bar{i}) & \bar{s}\frac{d}{di}\mathcal{R}(\bar{i}) - 1 \end{bmatrix} = \mathcal{R}_0 \begin{bmatrix} -\frac{\bar{i}}{1+\kappa(\bar{i})} & -\frac{\bar{s}(1+k(\bar{i})-\bar{i}\frac{d\kappa(\bar{i})}{d\bar{i}})}{(1+\kappa(\bar{i}))^2} \\ \frac{\bar{i}}{1+\kappa(\bar{i})} & \frac{\bar{s}(1+k(\bar{i})-\bar{i}\frac{d\kappa(\bar{i})}{d\bar{i}})}{(1+\kappa(\bar{i}))^2} - \frac{1}{\mathcal{R}_0} \end{bmatrix}. \quad (12)$$

At the equilibrium $E = (\bar{s}, 0, \bar{r})$, because $\kappa(0) = 0$ by assumption, J is identical to the Jacobian of the SIR model:

$$J_0 = \begin{bmatrix} 0 & -\bar{s} \\ 0 & \mathcal{R}_0 \bar{s} - 1 \end{bmatrix},$$

which is a stable matrix for any value of $\mathcal{R}_0 \geq 0$ as long as $\mathcal{R}_0 \bar{s} < 1$ (at equilibrium it must be true that $\mathcal{R}_0 \bar{s} < 1$). \square

Note that by assuming different nonlinear transmission rates, and including birth, death, and reinfection rates, *endemic* equilibria may emerge in which the equilibrium infectious population is positive, and bifurcations may occur (Liu et al., 1987; Hethcote, 2000; Korobeinikov and Maini, 2005).

2.3.2 Analysis of the solutions: advantages and disadvantages of infection-based feedback

By assuming that the derivative of the nonlinear transmission rate $\mathcal{R}(i)$ is bounded and has a maximum at $i = 0$, (Capasso and Serio, 1978) demonstrate global positivity, uniqueness, and global stability of the solutions for the fSIR model; these

results can be extended to similar models that include birth, death, and reinfection rates, and assumptions on the transmission rate can be relaxed as reviewed in (Korobeinikov, 2006). Here $\kappa(i)$ is assumed to be non-decreasing, and zero for $i = 0$, yielding a nonlinear transmission rate that is non-increasing and equal to \mathcal{R}_0 for $i = 0$ (Korobeinikov, 2006). In this case, it is shown that the peak of infections is always reduced in the presence of distancing. I will also summarize results that exist for the case in which the mitigation function is linear ($\kappa(i) = \kappa \cdot i$), and provide some additional qualitative result in regards to the time at which the infection peak occurs.

Problem 1 *The fSIR model (10)-(11) with initial conditions $s_0 \geq 0$, $i_0 > 0$, $r_0 \geq 0$, and $s_0 \mathcal{R}_0 > 1 + \kappa(i_0)$ defines an initial value problem (IVP) with non-negative solutions. We assume the mitigation function $\kappa(i)$ is a non-negative, non-decreasing function with $\kappa(0) = 0$, and we look for properties of the solutions of this IVP that hold for any \mathcal{R}_0 . These properties will be contrasted to the limit case $\kappa(i) = 0$ that corresponds to the IVP defined by the SIR model (4)-(5).*

The solution for $\kappa(i) = 0$ as well as its features will be denoted with the superscript 0 (i.e. if $\kappa(i) = 0$, $i^0(\tau) = i(\tau)$).

Nonlinear mitigation function: In the general case of a nonlinear mitigation function $\kappa(i)$, I will show that the peak of infections in the fSIR model is smaller than the infection peak for the SIR model, for any non-negative $\kappa(i)$; to the best of my knowledge, this is a novel result. No assumption is needed on the boundedness of the derivative of $\kappa(i)$ like in (Capasso and Serio, 1978).

Proposition 2 *In Problem 1, for any \mathcal{R}_0 and for any $\kappa > 0$, we have:*

$$i_{max} < i_{max}^0.$$

Proof Following the same approach used to derive (7), the peak of infection for the fSIR model can be estimated as follows:

$$\frac{di}{ds} = -1 + \frac{1 + \kappa(i)}{\mathcal{R}_0 s}.$$

We then obtain the infinitesimal expression:

$$di = -ds + \frac{ds}{\mathcal{R}_0 s} + \kappa(i) \frac{ds}{\mathcal{R}_0 s}, \quad (13)$$

in which the last term cannot be easily integrated, but it can be replaced by a simpler expression. Rearranging the terms of the ODE (10) we find:

$$\frac{1}{\mathcal{R}_0} \frac{ds}{s} = -\frac{i}{1 + \kappa(i)} d\tau,$$

which can be substituted in the last term of equation (13):

$$di = -ds + \frac{ds}{\mathcal{R}_0 s} - i \frac{\kappa(i)}{1 + \kappa(i)} d\tau,$$

thus we obtain the expression:

$$i = s_0 + i_0 - s + \frac{1}{\mathcal{R}_0} \log \frac{s}{s_0} - \int_0^\tau i \frac{\kappa(i)}{1 + \kappa(i)} d\sigma, \quad (14)$$

The infection peak occurs at $s_{crit} = (1 + \kappa(i_{max}))/\mathcal{R}_0$, which can be substituted in equation (14):

$$\begin{aligned} i_{max}(\tau_{max}) &= s_0 + i_0 - \frac{1 + \kappa(i_{max})}{\mathcal{R}_0} + \\ &+ \frac{1}{\mathcal{R}_0} \log \left(\frac{1 + \kappa(i_{max})}{\mathcal{R}_0 s_0} \right) - \int_0^{\tau_{max}} i \frac{\kappa(i)}{1 + \kappa(i)} d\sigma. \end{aligned} \quad (15)$$

When $\kappa(i) = 0$ we recover the original SIR infection peak expression (7), here denoted as i_{max}^0 . The difference between the peak value (15) and i_{max}^0 (the peak when $\kappa(i) = 0$) is:

$$\begin{aligned} i_{max} - i_{max}^0 &= -\frac{1}{\mathcal{R}_0} (\kappa(i_{max}) - \log(1 + \kappa(i_{max}))) - \\ &- \int_0^{\tau_{max}} i \frac{\kappa(i)}{1 + \kappa(i)} d\sigma. \end{aligned}$$

Because $\log(1 + x) < x$ for any $x > 0$, and because the last integral is strictly positive, we conclude that $i_{max} < i_{max}^0$ for any $\kappa > 0$. \square

Corollary 1 *In Problem 1, the equilibrium of susceptible individuals \bar{s} is always lower bounded by the equilibrium \bar{s}^0 .*

Proof At equilibrium it must be that $\dot{i} = 0$, and equation (14) yields:

$$\log \frac{s_0}{\bar{s}} = \mathcal{R}_0(1 - \bar{s}) - \int_0^{\bar{\tau}} i \frac{\kappa(i)}{1 + \kappa(i)} d\sigma,$$

where $\bar{\tau}$ is the time it takes to reach equilibrium. The equilibrium $0 \leq \bar{s} \leq 1$ must satisfy this equation. If $\kappa(i) = 0$ for all i , we recover expression (8): the left side of the equation is a curve that decreases monotonically as a function of \bar{s} , and the right side of the equation is a line with slope $-\mathcal{R}_0$ and intercept \mathcal{R}_0 when $\bar{s} = 0$. If $\kappa(i) \neq 0$, the left side of the equation is unchanged. The right side is still a line with slope $-\mathcal{R}_0$, however it intercepts the y -axis at a point $b < \mathcal{R}_0$, because the integral term is non-negative for any value of κ ; this is equivalent to shifting down the line. Thus, when $\kappa(i) \neq 0$, the intersection point \bar{s} of the curves on the left and right side of the equation intercept must be larger than the intersection when $\kappa(i) = 0$. \square

This proposition shows that, relative to an epidemic that lacks negative feedback, the fSIR model settles to a larger susceptible population in the disease-free equilibrium for any value of \mathcal{R}_0 and mitigation function. As a consequence, the equilibrium recovered population satisfies $\bar{r} < \bar{r}^0$.

Linear mitigation function: In the case of mitigation function linearly proportional to infections, $\kappa(i) = \kappa \cdot i$, the fSIR model can be solved exactly in phase space as demonstrated in (Capasso and Serio, 1978) and (Baker, 2020):

$$\frac{di}{ds} = -1 + \frac{1 + \kappa \cdot i}{\mathcal{R}_0 s},$$

terms can be rearranged to find an ordinary differential equation for $i(s)$:

$$s \frac{di}{ds} - \frac{\kappa}{\mathcal{R}_0} i(s) = -s + \frac{1}{\mathcal{R}_0}.$$

With the change of variable $z = \ln(s)$, we find:

$$\frac{di(z)}{dz} - \frac{\kappa}{\mathcal{R}_0} i(z) = -e^z + \frac{1}{\mathcal{R}_0},$$

which can be solved finding the phase-space expression:

$$i(s) = \left(i_0 + \frac{1}{\kappa} + \frac{\mathcal{R}_0}{\mathcal{R}_0 - \kappa} \right) s^{\frac{\kappa}{\mathcal{R}_0}} - \frac{1}{\kappa} - \frac{\mathcal{R}_0}{\mathcal{R}_0 - \kappa} s. \quad (16)$$

In the particular case when $\kappa = \mathcal{R}_0$, the solution is $i(s) = (s - 1)/\mathcal{R}_0 - s \ln s$. By setting $i(s) = 0$ one can find the final size of the susceptible population. By substituting $i_{max} = \frac{\mathcal{R}_0 s_{crit} - 1}{\kappa}$ in equation (16), one can derive s_{crit} :

$$s_{crit} = \frac{1}{\mathcal{R}_0} \left(i_0 \kappa (\mathcal{R}_0 - \kappa) + 1 + \kappa - \frac{\kappa}{\mathcal{R}_0} \right)^{\frac{1}{1 - \frac{\kappa}{\mathcal{R}_0}}}$$

and the corresponding infection peak can be found exactly; it can be verified that the infection peak always decreases with κ as predicted by Proposition 2.

To the best of my knowledge, an exact solution of fSIR with linear mitigation function has not been found. However, similar models with other particular forms of the nonlinear transmission rate can be solved exactly (Bohner et al., 2019).

I conjecture that in the presence of mitigation ($\kappa > 0$) the time at which the infection peak occurs is always delayed (although moderately) relative to the SIR model. While this conjecture is corroborated by numerical computations, a formal proof is left for future work.

2.4 Computational simulations

In these computational simulations I consider the fSIR model with linear mitigation function $\kappa(i) = \kappa \cdot i$ for illustrative purposes. It is assumed that κ remains constant unless otherwise noted.

Fig. 3, top, shows the numerically integrated solution of the fSIR model (10)-(11) with $\mathcal{R}_0 = 2.5$ as the parameter κ is varied. ($\mathcal{R}_0 = 2.5$ corresponds to a choice of $\beta = 0.25$ and $\gamma = 1/10$, i.e. the average time to recovery or death assumed to be 10 days; for comparison, the estimated average time to recovery in the COVID-19 epidemic is about 17 days for hospitalized patients (Zhou et al., 2020)). These

simulations confirm that the peak of infections decreases with a large κ , relative to the case $\kappa = 0$ (SIR without feedback). Fig. 3, bottom, shows the temporal evolution of the reproduction number in each simulation in the top panel: when infections increase, $\mathcal{R}(\tau)$ decreases; as infections decrease, $\mathcal{R}(\tau)$ converges to the nominal level ($\mathcal{R}_0 = 2.5$).

The duration of an epidemic is extended in the presence of mitigation

Simulations in Fig. 3 suggest that a large value of κ extends the duration of the epidemic. This is evident by examining an approximation of the fSIR solution (Problem 1): when κ is very large, thus $\kappa \cdot i \gg 1$, the fSIR can be approximated by the linear system:

$$\frac{d\hat{s}}{d\tau} \approx -\frac{\mathcal{R}_0}{\kappa}\hat{s}, \quad \frac{d\hat{i}}{d\tau} \approx \frac{\mathcal{R}_0}{\kappa}\hat{s} - \hat{i}. \quad (17)$$

The solution $\hat{i}(\tau)$ can be found exactly:

$$\hat{i}(\tau) = i_0 e^{-\tau} + s_0 \frac{\mathcal{R}_0}{\kappa - \mathcal{R}_0} \left(e^{-\tau} - e^{-\frac{\mathcal{R}_0}{\kappa}\tau} \right). \quad (18)$$

This approximation shows that if $\mathcal{R}_0/\kappa \ll 1$ the infection dynamics converge very slowly to $\hat{i} = 0$ (convergence is dominated by the constant \mathcal{R}_0/κ).

Simulations in Fig. 4 compare infections in a SIR and fSIR model with focus on the timescale of convergence to the disease-free equilibrium. Cumulative infections under the unmitigated epidemic are higher than in the mitigated case. However, the unmitigated epidemic extinguishes in about 6 months; in contrast, the infection-aware mitigation strategy maintains a significant level of infectious individuals for a much longer time. Further, after 3 years, the unmitigated epidemic cannot generate another outbreak ($\mathcal{R}_0 s < 1$), while the mitigated case may generate a new outbreak if social distancing and PPE were to be abandoned allowing \mathcal{R}_0 to return to its original value.

Infection-aware mitigation strategies reduce the peak of infection and do not postpone the peak significantly

The simulations in Fig. 3 confirm the results of Propositions 2, because the infection peak is always reduced. Additional simulations in Fig. 5 show that with a feedback parameter $\kappa = 2$ (taken as an illustrative value) the infection peak size can be reduced by about 30%, but this also causes a 30% extension of the time during which more than 2.5% of the population is infected. This is consistent with the observation made earlier that the duration of the epidemic is extended when adopting infection-dependent mitigation policies.

2.4.1 Effects of delayed infection awareness

Delays in detecting and reporting infections are to be expected (Li et al., 2020). While a theoretical analysis of the equilibria of the fSIR model with delays is not re-

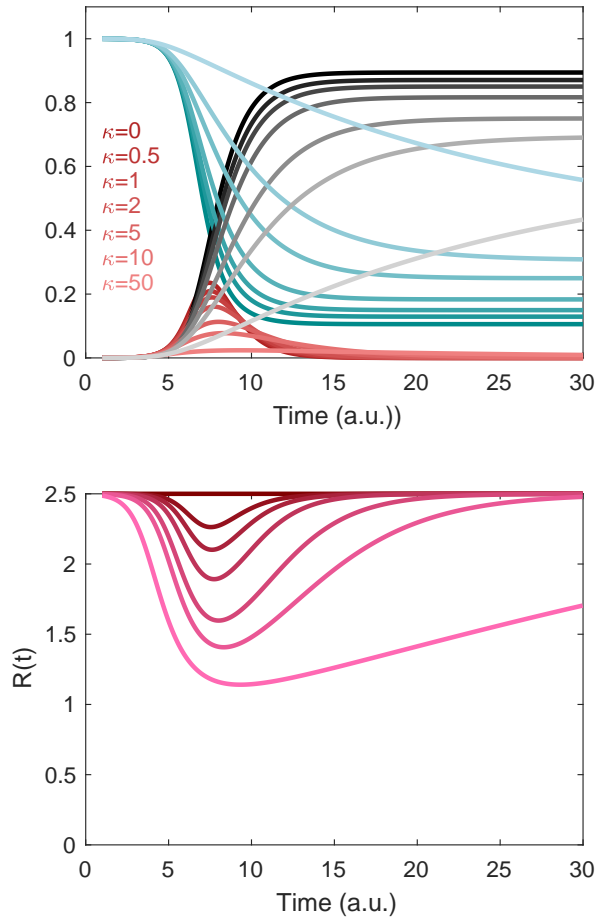


Figure 3: Numerically integrated solutions of the fSIR model. Top: Susceptible (green), infected (red), and recovered (gray) individuals when the parameter κ is varied (low to high, color shades from dark to light). Bottom: Evolution of the reproduction number in time computed from the simulations above; this can be interpreted as a qualitative measure of the implemented social distancing policies.

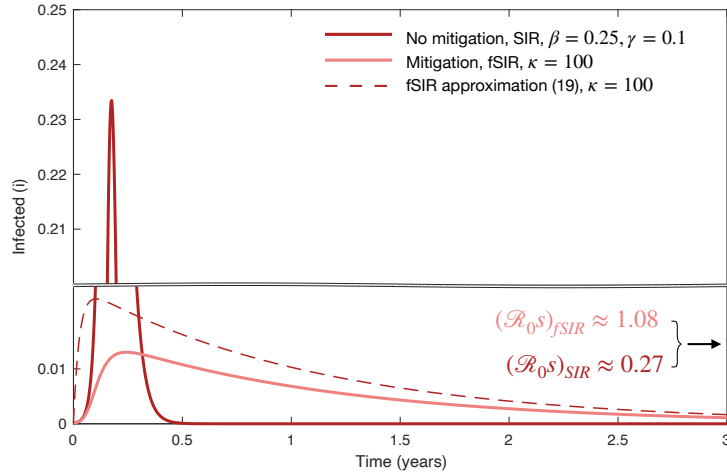


Figure 4: Mitigation based on infection awareness extends the duration of an epidemic ($\beta = 0.25$ and $\gamma = 0.1$). This simulation compares normalized infections in the SIR model with infections in the fSIR model ($\kappa = 100$), and the fSIR linear approximation (18). The y-axis is broken to emphasize the different timescale of convergence for SIR and fSIR. After 3 years, the SIR model does not admit a new outbreak; in contrast, if mitigation were to be completely relaxed ($\mathcal{R}_0 = 2.5$) the fSIR model could generate a new peak of infections because $\mathcal{R}_{0S} > 1$.

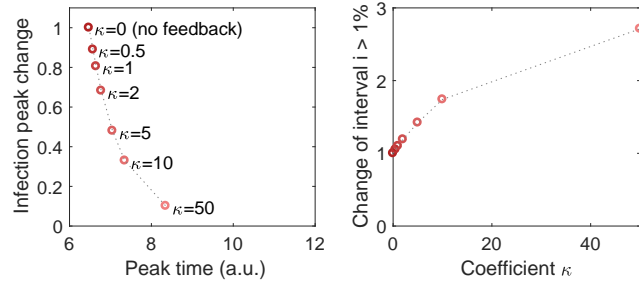


Figure 5: Left: Peak time versus peak value of infections for different values of the feedback parameter κ . This plot evidences that the peak is not delayed as in models where the transmission rate is constant and low. Right: The duration of infections is longer in the presence of feedback; here it is measured as the time interval for which the fraction of infected individuals is larger than 2.5% of the population.

ported here, it may be pursued using local or global methods used for very similar models in (Beretta and Takeuchi, 1995; Huang et al., 2010; Kyrychko and Blyuss, 2005; Kumar et al., 2020; Li and Liu, 2014). Rather, computational simulations are used here to examine whether a delay Δ in obtaining infection information can compromise the effects of mitigation feedback. A delay is included in the transmission rate expression:

$$\frac{ds}{d\tau} = -\mathcal{R}(i(\tau - \Delta))si, \quad \mathcal{R}(i(\tau - \Delta)) = \mathcal{R}_0 \frac{1}{1 + \kappa \cdot i(\tau - \Delta)}, \quad (19)$$

$$\frac{di}{d\tau} = (\mathcal{R}(i(\tau - \Delta))s - 1)i. \quad (20)$$

While stability of this model with delay is not examined here, global stability analysis of SIR models with nonlinear transmission and delays have been demonstrated in (Huang et al., 2010), and likely hold in this case.

For illustrative purposes, I choose a feedback parameter $\kappa = 2$ that remains fixed in these simulations, with $\mathcal{R}_0 = 2.5$ ($\beta = 0.25$ and $\gamma = 1/10$). Fig. 6 shows that a delay of up to 7 days increases the peak by less than 10%, but a 14 day delay causes a 25% increase in the peak, offsetting the peak reduction obtained by introducing feedback (the simulated non-dimensional delay is divided by the rescaling constant $\gamma = 1/10$).

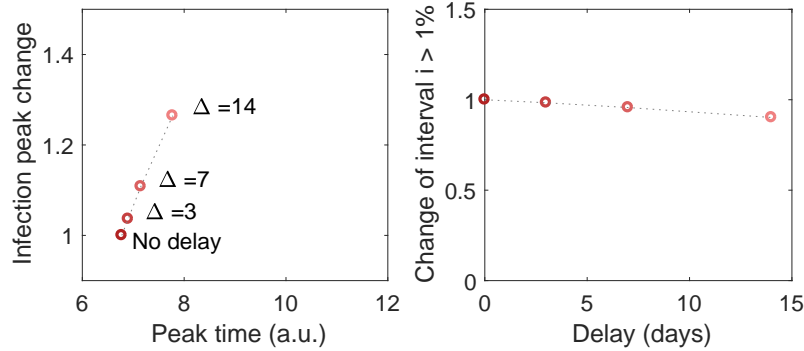


Figure 6: Effects of delays on the peak size and duration. Left: Change in peak size in the presence of delays, relative to the case in which feedback is present without delay and $\kappa = 2$. Right: The amount of time for which the fraction of infected population exceeds 2.5% is slightly reduced when delays are between 0 and 14 days.

2.4.2 The fSIR model captures the COVID-19 infection trends in the presence of mitigation strategies

The fSIR model was fitted to COVID-19 temporal series data for infections, recoveries, and deaths available from the Johns Hopkins Github repository (Dong

et al., 2020b), last accessed on July 15, 2020. I selected data from four western democracies: Italy, United Kingdom, Sweden, and the United States. The data were processed to compute active infections in a given day, and recoveries and deaths were summed and consolidated into the “recovered” compartment. All data were normalized by country population and thresholded to include only data collected after infections exceed 3 per million. Parameters were fitted with constraints $\beta \in [0 \ 0.6]$, $\beta \in [1/20 \ 1/10]$, and $\kappa \in [0 \ 10 \cdot 10^3]$; in the fitting score function, the infection prediction error was assigned a 100-fold penalty relative to the recovery data, with the expectation that recoveries may not be accurately reported for non-hospitalized patients. As a consequence, infection data are reproduced much more closely than recovery data by computationally generated trajectories that use fitted parameters.

Initial epidemic data in Italy, UK, Sweden, and the US are comparable, with reported infections and deaths showing similar doubling time of 2-4 days in the early (exponential) stages (Bertozzi et al., 2020). Mitigation or suppression measures were not *immediately* enacted, unlike countries such as South Korea, Japan, and Singapore that rapidly imposed lockdowns and contact tracing. (Timing and duration of initial interventions are critical for a successful containment (Sadeghi et al., 2020).)

Italy is an example country that, like Spain and France, imposed and enforced a strict suppression strategy (lockdown), which resulted in a very limited number of new infections as of June 2020. While also the UK officially imposed lockdown/stay-at-home orders, their enforcement appears to have been less successful than Italy, as shown in Fig. 7. From the beginning, Sweden followed a mitigation strategy relying on personal responsibility of citizens to limit the spread of the virus, rather than on a strict lockdown strategy. Finally, the US is an example of a federal state in which disparate containment approaches were enacted at different times, from a tight lockdown in some states like New York and Michigan, to loose mitigation policies in other states like Arizona, Texas, and Florida. Interestingly, infection data from both Sweden and the US show a trend change around the end of May 2020, which is marked qualitatively by a black line at day 90 in Fig. 8. Because the overall US data includes contributions from all states, the first phase is likely dominated by the major outbreaks and lockdowns in the north eastern states in March and April 2020, while the second phase is dominated by southern states that relaxed mitigation strategies in May 2020.

The fSIR model can not reproduce the infection data from Italy (in addition, the fitted transmission parameter β is unrealistically high, and so is \mathcal{R}_0). Italy’s COVID-19 reaction can be reproduced with a SIR model with a time-varying \mathcal{R}_0 tied to fluctuations in lockdown measures (Casella, 2020), that do not depend on infection levels (until new infections are nearly completely eliminated). In contrast, the fSIR model reproduces very well active infection trends in the UK, with realistic fitted parameters, suggesting that the UK lockdown measures were as effective as an infection-based mitigation strategy. The fitted value of $\kappa \approx 1107$ means that a substantial societal reaction (reduction of the transmission coefficient) occurred relatively late in the epidemic, roughly when 0.1% of the population was reported to be infected.

To fit infection data from the US and Sweden, we imposed single value of β and γ but allowed two distinct values of mitigation parameter κ to capture the two apparent phases of the outbreak. In both cases, the fitted values of β and γ are realistic, and the values of κ decrease in the second phase, suggesting that mitigation strategies were overall relaxed or that their effectiveness decreased over time.

Even though all these countries ramped up their testing efforts, actual infection data are always underestimated. For this reason, it is interesting to test changes in the fSIR fitted parameters assuming a larger number of individuals affected by the epidemic. If data are scaled by X -fold (*i.e.* infections and recoveries are believed to be X -times larger than reported), the fitted κ qualitatively scales by a factor $1/X$, while changes in fitted β and γ are negligible.

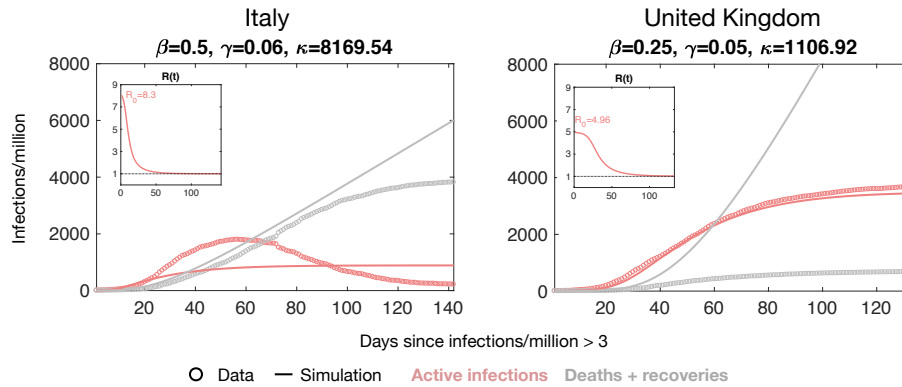


Figure 7: COVID-19 active infection and recovery/death data for Italy and the United Kingdom, fitted using the fSIR model; the reproduction coefficient $\mathcal{R}(t)$ is shown in the insets. The fSIR model cannot capture the Italian infection data, as strict lockdown policies were enacted and enforced without relaxation for a sufficiently long time; this scenario would be better captured by a nearly discrete change in the reproduction coefficient (Fig. 1C). In contrast, the fSIR model reproduces very well active infection data in the UK, with realistic estimates for the transmission rate and $\mathcal{R}(t)$. This suggests that in practice, the UK strategy may be classified as an infection-based mitigation approach. Data fitting details are in Section 2.4.2.

This data fitting exercise has largely an illustrative purpose, and is not meant to put forward any predictions. The pitfalls of relaxing mitigation policies too early are discussed in detail using many models that are more complex and accurate than the one presented here (Kissler et al., 2020; Giordano et al., 2020).

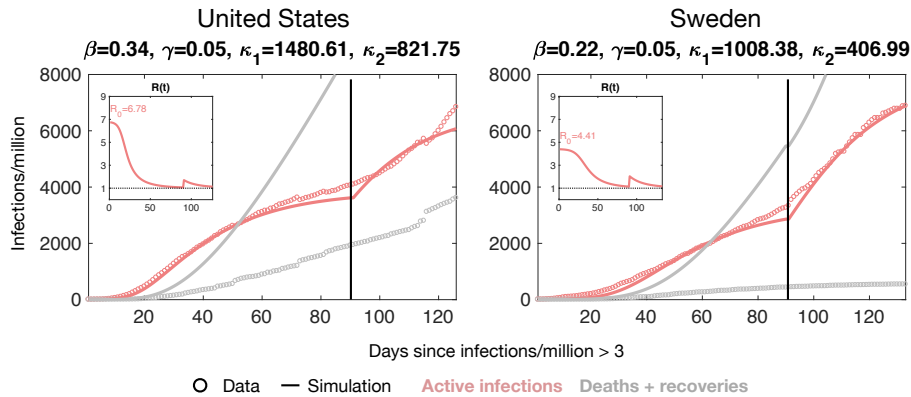


Figure 8: COVID-19 active infection and recovery/death data for Sweden and the overall United States, fitted using the fSIR model, with reproduction coefficient $\mathcal{R}(t)$ in the insets. The infection trend of both countries shows two distinct phases, which are qualitatively separated by the black line placed at day 90. The fSIR model reproduces the trends observed adopting a different value of κ in each phase (κ_1 for before day 90, κ_2 for after day 90). Data fitting details are in Section 2.4.2.

3 Conclusion

I have derived and examined the properties of a modified SIR model, here named feedback SIR (fSIR), in which infection-based mitigation policies introduce a reproduction number that decreases a continuous function of infection levels, generating a negative feedback loop. This simple model was originally described by (Capasso and Serio, 1978), and here it is derived from first principles by considering cases in which individuals reduce their contacts or use PPE as more infections are reported. Using a time-scale separation argument, it was shown that the transmission rate function takes the form of a Holling type II or Michaelis-Menten function popular in ecology, chemistry and biology. It was demonstrated that mitigation based on infection awareness always reduces the infection peak, but substantially lengthens the duration of the epidemic. In the special case of a mitigation function that is linear with respect to infection information, this model requires only one additional parameter to capture the effects of social distancing and is amenable to exact analysis (Baker, 2020). Extending the results presented here to an fSEIR model appears trivial, but is left for future work.

The reduction of transmission rate as a function of knowledge of infections, recoveries, or deaths goes beyond non-pharmacological mitigation strategies. While it is unlikely that vaccines for SARS-CoV-2 will be available before 2021, information about infection levels is likely to increase the likelihood of mass vaccination and thus cause a substantial decrease in the susceptible population; models like the one presented here may describe well this scenario (Bootsma and Ferguson, 2007; Kiss et al., 2010; Buonomo et al., 2008). As widespread access to real-time epidemic information is available, and contact tracing becomes prevalent, closed-

loop feedback regulation of epidemics is within reach. The role of nonlinear transmission parameters that introduce feedback is yet to be ascertained within more sophisticated compartment models developed for COVID-19 (Kissler et al., 2020; Giordano et al., 2020). While accurate forecasting will take advantage of complex models integrating data on multiple scales, simple models like the one presented here can provide general insights and guidelines to policymakers, doctors, and educators.

4 Methods

Differential equations were integrated with a forward Euler method in MATLAB using custom scripts, or using MATLAB's `ode45`. Data fitting was done using MATLAB's `fmincon`.

5 References

References

- C. Anastassopoulou, L. Russo, A. Tsakris, and C. Siettos. Data-based analysis, modelling and forecasting of the COVID-19 outbreak. *PLoS one*, 15(3):e0230405, 2020.
- R. M. Anderson and R. M. May. Regulation and stability of host-parasite population interactions: I. regulatory processes. *The journal of animal ecology*, pages 219–247, 1978.
- R. Baker. Reactive social distancing in a SIR model of epidemics such as COVID-19. *arXiv preprint arXiv:2003.08285*, 2020.
- E. Beretta and Y. Takeuchi. Global stability of an SIR epidemic model with time delays. *Journal of mathematical biology*, 33(3):250–260, 1995.
- A. L. Bertozzi, E. Franco, G. Mohler, M. B. Short, and D. Sledge. The challenges of modeling and forecasting the spread of covid-19. *Proceedings of the National Academy of Sciences*, 2020. doi: 10.1073/pnas.2006520117.
- M. Bin, P. Cheung, E. Crisostomi, P. Ferraro, C. Myant, T. Parisini, and R. Shorten. On fast multi-shot epidemic interventions for post lock-down mitigation: Implications for simple COVID-19 models. *arXiv preprint arXiv:2003.09930*, 2020.
- M. Bohner, S. Streipert, and D. F. Torres. Exact solution to a dynamic SIR model. *Nonlinear Analysis: Hybrid Systems*, 32:228–238, 2019.
- M. C. Bootsma and N. M. Ferguson. The effect of public health measures on the 1918 influenza pandemic in US cities. *Proceedings of the National Academy of Sciences*, 104(18):7588–7593, 2007.

- B. Buonomo, A. d'Onofrio, and D. Lacitignola. Global stability of an SIR epidemic model with information dependent vaccination. *Mathematical biosciences*, 216(1):9–16, 2008.
- G. C. Calafiore, C. Novara, and C. Possieri. A time-varying SIRD model for the COVID-19 contagion in italy. *Annual reviews in control*, 2020.
- V. Capasso and G. Serio. A generalization of the Kermack-McKendrick deterministic epidemic model. *Mathematical Biosciences*, 42(1-2):43–61, 1978.
- F. Casella. Can the COVID-19 epidemic be managed on the basis of daily data? *arXiv preprint arXiv:2003.06967*, 2020.
- M. Chapwanya, J. M.-S. Lubuma, and R. E. Mickens. From enzyme kinetics to epidemiological models with Michaelis–Menten contact rate: Design of nonstandard finite difference schemes. *Computers & Mathematics with Applications*, 64(3):201–213, 2012.
- J. Dawes and M. Souza. A derivation of Holling's type i, ii and iii functional responses in predator–prey systems. *Journal of theoretical biology*, 327:11–22, 2013.
- F. Della Rossa, D. Salzano, A. Di Meglio, F. De Lellis, M. Coraggio, C. Calabrese, A. Guarino, R. Cardona-Rivera, P. De Lellis, D. Liuzza, et al. A network model of italy shows that intermittent regional strategies can alleviate the COVID-19 epidemic. *Nature communications*, 11(1):1–9, 2020.
- E. Dong, H. Du, and L. Gardner. An interactive web-based dashboard to track COVID-19 in real time. *The Lancet*, 2020a. <https://plague.com/>.
- E. Dong, H. Du, and L. Gardner. An interactive web-based dashboard to track COVID-19 in real time. *The Lancet infectious diseases*, 2020b.
- S. Funk, E. Gilad, C. Watkins, and V. A. Jansen. The spread of awareness and its impact on epidemic outbreaks. *Proceedings of the National Academy of Sciences*, 106(16):6872–6877, 2009.
- G. Giordano, F. Blanchini, R. Bruno, P. Colaneri, A. Di Filippo, A. Di Matteo, and M. Colaneri. Modelling the COVID-19 epidemic and implementation of population-wide interventions in italy. *Nature Medicine*, pages 1–6, 2020.
- D. Greenhalgh, S. Rana, S. Samanta, T. Sardar, S. Bhattacharya, and J. Chattopadhyay. Awareness programs control infectious disease–multiple delay induced mathematical model. *Applied Mathematics and Computation*, 251:539–563, 2015.
- T. Harko, F. S. N. Lobo, and M. K. Mak. Exact analytical solutions of the susceptible–infected–recovered (SIR) epidemic model and of the SIR model with equal death and birth rates. *Applied Mathematics and Computation*, 236:184–194, 2014.

- H. W. Hethcote. Qualitative analyses of communicable disease models. *Mathematical Biosciences*, 28(3-4):335–356, 1976.
- H. W. Hethcote. The mathematics of infectious diseases. *SIAM review*, 42(4): 599–653, 2000.
- G. Huang, Y. Takeuchi, W. Ma, and D. Wei. Global stability for delay SIR and SEIR epidemic models with nonlinear incidence rate. *Bulletin of mathematical biology*, 72(5):1192–1207, 2010.
- W. O. Kermack and A. G. McKendrick. A contribution to the mathematical theory of epidemics. *Proceedings of the royal society of london. Series A, Containing papers of a mathematical and physical character*, 115(772):700–721, 1927.
- I. Z. Kiss, J. Cassell, M. Recker, and P. L. Simon. The impact of information transmission on epidemic outbreaks. *Mathematical biosciences*, 225(1):1–10, 2010.
- S. M. Kissler, C. Tedijanto, E. Goldstein, Y. H. Grad, and M. Lipsitch. Projecting the transmission dynamics of SARS-CoV-2 through the postpandemic period. *Science*, 2020.
- T. Kolokolnikov and D. Iron. Law of mass action and saturation in SIR model with application to coronavirus modelling. *Infectious Disease Modelling*, 2020.
- A. Korobeinikov. Lyapunov functions and global stability for SIR and SIRS epidemiological models with non-linear transmission. *Bulletin of Mathematical biology*, 68(3):615, 2006.
- A. Korobeinikov and P. K. Maini. Non-linear incidence and stability of infectious disease models. *Mathematical medicine and biology: a journal of the IMA*, 22(2):113–128, 2005.
- T. Kruse and P. Strack. Optimal control of an epidemic through social distancing. 2020.
- A. J. Kucharski, T. W. Russell, C. Diamond, Y. Liu, J. Edmunds, S. Funk, and R. M. Eggo. Early dynamics of transmission and control of covid-19: a mathematical modelling study. *The Lancet, Infectious Diseases*, 2020. March 11, 2020.
- A. Kumar, K. Goel, et al. A deterministic time-delayed SIR epidemic model: mathematical modeling and analysis. *Theory in Biosciences*, 139(1):67–76, 2020.
- Y. N. Kyrychko and K. B. Blyuss. Global properties of a delayed SIR model with temporary immunity and nonlinear incidence rate. *Nonlinear analysis: real world applications*, 6(3):495–507, 2005.
- G.-H. Li and Y.-X. Zhang. Dynamic behaviors of a modified SIR model in epidemic diseases using nonlinear incidence and recovery rates. *PLoS One*, 12(4): e0175789, 2017.

- M. Li and X. Liu. An sir epidemic model with time delay and general nonlinear incidence rate. In *Abstract and Applied Analysis*, volume 2014. Hindawi, 2014.
- R. Li, S. Pei, B. Chen, Y. Song, T. Zhang, W. Yang, and J. Shaman. Substantial undocumented infection facilitates the rapid dissemination of novel coronavirus (SARS-CoV-2). *Science*, 368(6490):489–493, 2020.
- W.-m. Liu, S. A. Levin, and Y. Iwasa. Influence of nonlinear incidence rates upon the behavior of SIRS epidemiological models. *Journal of mathematical biology*, 23(2):187–204, 1986.
- W.-m. Liu, H. W. Hethcote, and S. A. Levin. Dynamical behavior of epidemiological models with nonlinear incidence rates. *Journal of mathematical biology*, 25(4): 359–380, 1987.
- B. Prasse, M. A. Achterberg, L. Ma, and P. V. Mieghem. Network-based prediction of the 2019-ncov epidemic outbreak in the chinese province hubei, 2020. <https://arxiv.org/pdf/2002.04482.pdf>.
- U. Rosini. COVID-19 Italia - Monitoraggio situazione, 2020. GitHub repository of data from Italy COVID-19 epidemic <https://github.com/pcm-dpc/COVID-19>.
- M. Sadeghi, J. Greene, and E. Sontag. Universal features of epidemic models under social distancing guidelines. *bioRxiv*, 2020.
- S. Samanta and J. Chattopadhyay. Effect of awareness program in disease outbreak—a slow–fast dynamics. *Applied Mathematics and Computation*, 237: 98–109, 2014.
- G. Stewart, K. Heusden, and G. A. Dumont. How control theory can help us control COVID-19. *IEEE Spectrum*, 57(6):22–29, 2020.
- J. S. Weitz, S. J. Beckett, A. R. Coenen, D. Demory, M. Dominguez-Mirazo, J. Dushoff, C.-Y. Leung, G. Li, A. Măgălie, S. W. Park, et al. Modeling shield immunity to reduce COVID-19 epidemic spread. *Nature medicine*, pages 1–6, 2020.
- D. Yu, Q. Lin, A. P. Chiu, and D. He. Effects of reactive social distancing on the 1918 influenza pandemic. *PloS one*, 12(7), 2017.
- F. Zhou, T. Yu, R. Du, G. Fan, Y. Liu, Z. Liu, J. Xiang, Y. Wang, B. Song, X. Gu, et al. Clinical course and risk factors for mortality of adult inpatients with covid-19 in wuhan, china: a retrospective cohort study. *The Lancet*, 2020.